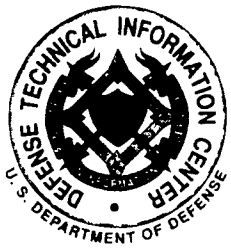

Defense Technical Information Center Compilation Part Notice

This paper is a part of the following report:

• *Title:* Technology Showcase: Integrated Monitoring, Diagnostics and Failure Prevention. Proceedings of a Joint Conference, Mobile, Alabama, April 22-26, 1996.

• *To order the complete compilation report, use:* AD-A325 558

The component part is provided here to allow users access to individually authored sections of proceedings, annals, symposia, etc. However, the component should be considered within the context of the overall compilation report and not as a stand-alone technical report.

OVERVIEW OF WAVELET / NEURAL NETWORK FAULT DIAGNOSTIC METHODS APPLIED TO ROTATING MACHINERY

Jose E. Lopez
Inna A. Farber Yeldham
Kevin Oliver
ALPHATECH, Inc.
50 Mall Road
Burlington, MA 01803-4562

Abstract: New technology in the form of wavelet-based methods coupled with intelligent classification schemes built around neural networks, can drive the development of substantially improved fault detection and identification (FDI) methods. Such systems represent important next generation FDI kernels for integration into advanced condition based maintenance systems for rotating machinery. This paper presents an overview of the results obtained by ALPHATECH in a program aimed at developing wavelet/neural network based FDI systems for vibrating machinery. The paper presents the performance results of these methods applied to a range of platforms including helicopter transmissions, turbopumps, and gas turbines. In addition, enhancements to the basic fault detection and identification system are presented and include overviews of multi-sensor wavelet-based differential features and improved FDI performance through classification fusing using hierarchical neural networks.

Key Words: monitoring; rotating machinery; fault detection; helicopter transmissions; prognosis; condition based maintenance; wavelets; neural networks

INTRODUCTION: As the 21st century approaches, global competition will continue to produce tremendous economic pressures on all industrial powers. The results of this competition are shorter time to market and thinning profit margins with a simultaneous demand for increased product quality and improved overall efficiency. Unfortunately, the coupling of these phenomena to military domains will be quite direct. Decreases in real GNP for individual industrial powers directly affects their ability/determination for increasing resources for maintaining viable high-tech military forces in an ever increasing complex world. The military domain under such circumstances will continue to experience increasingly tighter budget appropriations, cancellation of important new systems while simultaneously struggling with the problems of sustaining a high state of readiness in the face of rapidly aging platforms.

In the commercial domain, knowledge of enterprise wide machinery health and usage are crucial to avoid expensive down time. Timely fault detection and identification at a local level can prevent more serious damage to other parts of the enterprise that are coupled. In the military domain, the mathematics of decreased budgets translates to being able to maintain the status quo with fewer resources. For personnel intensive operations, methods for streamlining processes, increasing automation, and computerizing monitoring/reporting will be at the top of the priority list. More sophisticated/automated machine monitoring systems that require reduced human intervention will be a very desired commodity.

Presently, the dramatic decrease in the cost of powerful computational capability is fueling the investigation and uses of significantly more advanced system and signal processing methods for application to the domain of machine monitoring and prognostic systems [1]-[3]. A particularly promising set of methods relies on the application of wavelets and neural networks to the development of next generation fault detection and identification (FDI) systems [4]-[12]. The current form of the technology involves wavelet-based methods for decomposing system vibrations and coupling intelligent classification schemes that rely on neural networks for identifying machine condition and state of deterioration.

This paper presents an overview of these wavelet/neural network based FDI methods. The paper presents the performance results of these methods applied to a range of platforms, such as helicopter transmissions, turbopumps, and gas turbines. Additionally, enhancements to the basic fault detection and identification system are presented and include overviews of multi-sensor wavelet-based differential features and improved FDI performance through classification fusing using hierarchical neural networks.

WAVELET/NEURAL NETWORK BASED METHODS: This section presents the application of wavelet-based techniques coupled with neural networks to develop a fault detection and identification system. Continuous wavelet transforms and the selection of wavelet basis functions appropriate for real-time feature extraction are discussed. Examples are given for complex platforms providing formidable FDI challenges. The successful development of advanced fault monitoring processes for these platforms provides substantial benchmarks for the viability of the wavelet-based tools being developed.

Continuous Wavelet Transforms: To develop viable FDI schemes, means of extracting significant discriminate features from the vibration signal plays a critical role. Harmonic analyses in the form of a Fourier transform proves problematic for several reasons. First, the transform is global in that localized events in time can affect the entire frequency spectrum. Additionally, the Fourier transform is fundamentally not applicable to real-time monitoring applications due to the mathematical formulation of the transform that operates on the entire time axis. Windowing schemes are thus required to address the real-time feature extraction requirements for capturing important events localized in time. Unfortunately, fixed windowing schemes imply fixed time-frequency resolution in the time-frequency plane. The problem this poses is the selection of a single window that provides sufficient fidelity discriminating important events in the vibration signal that are separated by large orders of magnitude along the frequency axis. This scenario is exemplified by main helicopter transmissions where important information concerning bearings can be on the order of tens to hundreds of Hertz, whereas mesh frequencies and important fundamentals associated with gearing of the engine inputs can be on the order of tens of thousands of Hertz (i.e. order of $\sim 10^4$).

The continuous wavelet transform (CWT) resolves the window selection problem with a "zoom-in" and "zoom-out" capability that generates a flexible time-frequency window that automatically narrows (along the time axis) at high center-frequencies and expands (along the time axis) at low center frequencies [13]. The continuous wavelet transform provides this flexible time-frequency analysis by decomposing the vibration signal over dilated and translated wavelet basis functions. A wavelet is a function with finite energy, or a member of the function space $L^2(R)$, i.e., a wavelet function satisfies:

$$\int_{-\infty}^{\infty} |\psi(x)|^2 dx < \infty \tag{1}$$

The wavelet function has a zero average or essentially no DC component. A set of basis functions is obtained through dilation's and translations of a base wavelet and takes the form:

$$\psi_{u,s}(t) = \frac{1}{\sqrt{s}} \psi\left(\frac{t-u}{s}\right) \tag{2}$$

where u is the translation parameter and s is the dilation parameter. The wavelet transform is then achieved via the inner product of the respective vibration signal, $f(t)$, with the wavelet basis function of eq. (2):

$$W_\psi f(u,s) = \int_{-\infty}^{\infty} f(t) \frac{1}{\sqrt{s}} \psi^*\left(\frac{t-u}{s}\right) dt \tag{3}$$

There are an infinite number of wavelet basis functions that satisfy eq. (1) and contain no DC component. The particular analyzing wavelet basis functions used in this work were mathematically inspired from biological systems that are effective in their decomposition and detection of vibration signals. The wavelet basis functions mimic the auditory nerve neuron's impulse response. This particular wavelet family has semi-infinite support in the time domain and can be modeled using causal real-rational transfer functions. The immediate implication is the ability to develop, on the individual wavelet basis function level, real-time feature extractors that can be efficiently implemented using auto-regressive moving average techniques (ARMA).

Wavelet-Based FDI: Figure 1 provides a simplified block diagram of a wavelet-based FDI system. The goal of the system is two-fold. First, the wavelet-based feature extraction provides the important role of extracting the essential projections of the system dynamics in an efficient manner. Second, the wavelet feature set essentially reduces the dimension of the information from the input space (real-time, continuous, analog vibration signal) to a robust lower dimensional representation that simplifies the design of the adaptive neural network classification scheme. In the design phase (as indicated in Figure 1), CWT analysis is performed on the vibration data sets to identify a set of robust wavelet features (in time and frequency) that provide discrimination between normal operation and failure conditions. In addition, these wavelet features provide sufficient separation of the failure conditions in feature space for reliable identification of the fault condition using capable classification technologies such as neural networks. Once selected, these features form the components of a feature vector extracted from the vibration signal on a regular basis. The time interval between wavelet-based feature vectors extracted from the vibration signal is user and application dependent [6].

As part of the extraction process, the wavelet basis function is adapted relative to slowly varying mesh fundamentals to compensate for input engine RPM fluctuations. Feature post-processing in the form of nonlinear transformations of the feature components is employed to provide enhanced separation of failure conditions in feature space, and hence improved classification. Finally, extracted feature vectors train an adaptive, neural network classifier. During real-time monitoring applications, the classifier output provides basic/raw classification results indicating the state of the system under test. Depending on the actual system requirements and needs, this basic classification information may be subject to further processing to enhance higher level diagnostic decision systems, or may be conjoined with other auxiliary information or systems in a fully integrated diagnostic/intelligent monitoring system.

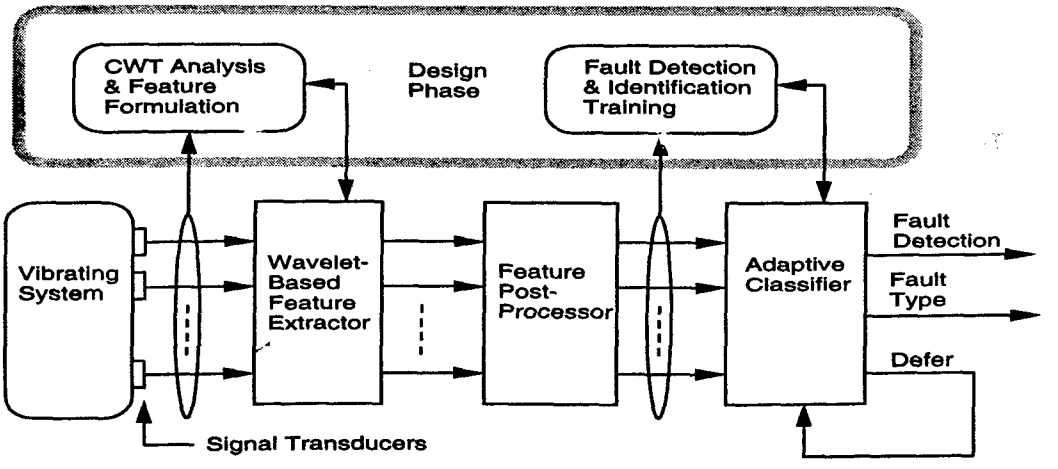

Figure 1. Wavelet-based FDI System

APPLICATION TO ROTATING MACHINERY:

Helicopter Main Transmission: Data sets from the main transmission of a helicopter with seeded faults were acquired from a major helicopter manufacturer. The transmission involves multiple gears, multiple shafts, and multiple meshes, and thus produces complex vibration data. The challenge is determining the physical phenomena that can be inferred from the wavelet visualizations, and whether a robust feature set can be extracted for FDI purposes. It is necessary to relate the CWT visualization structure to physical phenomena when selecting wavelet based features. Despite the complexity of the vibration structure in this helicopter main transmission, the CWT provides a vivid portrayal of the physical phenomenon occurring during the transmission operation.

CWT Analysis Main Transmission: Figure 2 is a CWT visualization of the first second of normal operation of the helicopter main transmission as recorded by a sensor on the transmission housing [9] at a shaft input power of 1000 HP. The Figure 2 visualization contains 512 wavelet filters distributed in an octave (log base 2) fashion along the scale axis (the vertical axis with units of Hz). The magnitude of the wavelet outputs were processed by a smoothing filter configured to have 5 millisecond smoothing time constant. The outputs were down-sampled to 512 Hz and the magnitudes color-coded using a hue-saturation scheme that maps red to large magnitudes and black to small magnitudes.

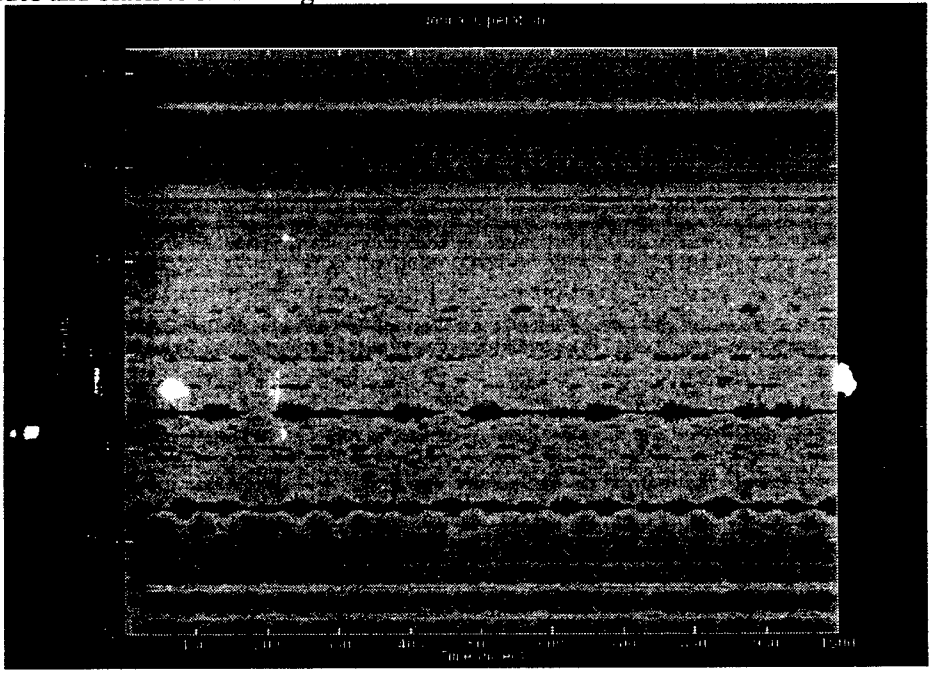

Figure 2. CWT of Normal Operation for Helicopter Transmission

The most notable structure in Figure 2 is the frequency-modulated and amplitude-modulated structure at around 1323 Hz. This corresponds to the mesh between the main input bevel gear and the top of the main bevel gear. This modulation is a very common effect in the vibrations of drive systems [14], and is usually (but not always) related to the shaft frequency. For the CWT of Figure 2, the average modulation period is of the order of approximately 52 milliseconds. This corresponds to a frequency of 19.2 Hz, which is nearly the frequency of rotation of the Main Bevel Gear. The second harmonic of the mesh at 1323 Hz is once again very visible at approximately 2646 Hz and exhibits a smearing effect of the modulation observed in the

fundamental. The third fundamental at 3969 Hz is still very visible. Another important vibration at 12920 Hz is prominent in Figure 2. This vibration corresponds to the mesh of the input engines and spur gears. The second harmonic of this mesh is also visible at 25840 Hz. A modulated vibration at approximately 1949 Hz corresponds to the mesh of the bottom of the main bevel gear and main bevel output gear to the tail rotor. The lines associated with the second harmonic are readily visible at 3898 Hz. There is a relatively strong line at approximately 5708 Hz, and it's second and third harmonics appear visible at 11416 Hz and 17124 Hz, respectively.

To determine a viable set of robust wavelet features, the normal operation CWT must be compared against the CWT visualizations for all fault cases. Additional processing tools based on morphological operations of the CWT images assist the feature identification process. The selection is primarily data driven (i.e., driven by differences detected in the visualizations), but the analysis of the previous section provides important links to the physics of the vibration structure observed. This ensures the capturing of important system dynamics that bear a causal relation to the underlying physics of the fault vibration mechanisms.

Extracted features were normalized by the magnitude of the wavelet output associated with the linking feature to account for recording variation. The wavelet magnitude outputs were smoothed using a 5 millisecond smoothing time constant and features were extracted every 10 milliseconds. Features were extracted from approximately 2.9 seconds of data for each case, and each case generated 286 feature vectors. More details concerning the features extracted and feature post processing are found in [9].

Neural Network Classification and Results: A total of 858 feature vectors (286 from each of three classes: normal, pre-overhaul, and post-overhaul) resulted from the feature extraction process. Three hundred (300) feature vectors, or 100 from each class, were used to train a global neural network with backpropagation. The neural network was trained until a sum-squared error of .975 was attained. Once the neural network was trained, all 858 feature vectors were presented to the neural network for classification. The performance results appear in Table 1. The cost of obtaining this extremely accurate classification is modest. The neural networks consisted of a small number neurons. The relative training time and convergence to small sum-squared errors was very fast given the small number of neurons used.

TABLE 1. SUMMARY OF NEURAL NETWORK PERFORMANCE RESULTS

Performance Results	
Prob. of False Alarm	.00699
Prob. of Missed Detection	.00350
Prob. of Misclassification	.00466
Prob. of Deferral	0
Number of Feature Vectors Used in Training	300

Performance Results	
Number of Feature Vectors Used in Classification	858
Number of layers	1
Number of total Neurons	3
Training Error (SSE)	.975838
Number of Training Epochs	8550

Complete Non-Parametric Approach: To illustrate that one can build wavelet-based FDI systems with essentially no detailed mechanical information concerning the underlying platforms, a second set of vibrational data from a different helicopter transmission was obtained. Unlike the previous helicopter example, this helicopter data set was unaccompanied by any mechanical information. The goal was thus to apply our wavelet methodology to develop a high performing FDI system in the absence of any detailed mechanical information.

The data was supplied with the following brief information: vibration data for normal operation ("nor") and multiple fault conditions were recorded at different torque levels by eight accelerometers positioned at various unspecified locations. The multiple fault operations included bearing corrosion at the planetary pinion ("fault 2") and at the spiral bevel input pinion ("fault 3"), tooth spalling at the spiral bevel input pinion ("fault 4"), tooth chipping at the helical input pinion gear ("fault 5"), and crack propagation at the helical idler gear ("fault 6"), at the collector gear ("fault 7") and at the quill shaft ("fault 8"). The data from the eight accelerometer sites was multiplexed with a reference and tachometer signal. Each signal contained 2.261 million samples with a 116.5 kHz sampling rate. No mechanical information was provided.

An initial approach consisted of selecting an intermediate torque setting. Not every fault was recorded at every torque level. Therefore, an intermediate torque value with a representative number of faults was selected. CWT visualizations were then generated at all accelerometer sites to identify the most observable sites. Accelerometer 7 was selected as the most desirable accelerometer site and CWT analysis was performed using the data for 100% torque values that included normal condition and six (out of seven) fault conditions.

Discriminating features were obtained by comparing the normal and fault operation CWTs. These features were then used to train a global neural network. The neural network architecture used a backpropagation learning rule with an adaptive learning rate and momentum. The neural network consisted of two layers and twenty-two neurons (fourteen neurons in the first layer, eight neurons in the output layer). The network was deemed trained when a sum squared error of 0.02 was achieved. The data for the fault scenarios and the normal condition at accelerometer site seven at 100% torque was then applied to the neural network for classification.

A confusion matrix is presented in Table 2. The network trained on 100 feature vectors and classified 920 feature vectors. Wavelet-based feature vectors were extracted every 10 ms. To understand the tabulation method (i.e., confusion matrix) used to display the results of this FDI simulation, individual table elements indicate the following: an element in the confusion matrix indicates the number of feature vectors from a given class (row label) that were classified as the class with the corresponding column label. Perfect fault detection and identification results in a confusion matrix tabulation were all numbers aligned on the main diagonal.

Results as tabulated in Table 2 indicate that very high performing wavelet/neural network based FDI was obtained. The probability of false alarm was zero and the probability that a fault condition will be classified as normal operation is 0.078%. The probability of fault misclassification is 0.068%.

FDI analysis was therefore successfully performed non-parametrically. Mechanical information about the helicopter transmission system was unknown and the only information supplied was the number and types of faults present in the transmission. A feature set was derived merely by comparing CWT visualizations from normal and fault operation. This generic methodology was then used to generate feature vectors that trained a global neural network. The classification performance of the neural network was highly accurate as shown by the confusion matrix and the time history of the neural network performance.

Turbopump Applications: This section focuses on applications of the wavelet based FDI system to detect bearing failures within High Pressure Oxygen Turbopumps (HPOTP) of the Space Shuttle Main Engine (SSME). The SSME turbopump rotates at up to 30,000 rpm on two pairs of bearings, one pair at the pump end and one pair at the turbine end.

Vibration data was collected during several test firings at two different rated power levels (104% and 109%) of one new turbopump and six faulty turbopumps (i.e., these pumps were rejected by the flight center due to the evidence of bearing degradation in their dynamic signatures). The

TABLE 2. WAVELET / NEURAL NETWORK BASED FDI SIMULATION RESULTS

	Estimated Classes								
Correct Classes	nor	fault 2	fault 3	fault 4	fault 5	fault 6	fault 7	fault 8	def
nor	920	0	0	0	0	0	0	0	0
fault 2	0	920	0	0	0	0	0	0	0
fault 3	0	0	920	0	0	0	0	0	0
fault 4	0	0	0	920	0	0	0	0	0
fault 5	0	0	0	0	920	0	0	0	0
fault 6	5	0	0	0	0	915	0	0	0
fault 7	0	0	0	0	0	0	920	0	0
fault 8	0	0	0	0	0	0	0	920	0

vibration signals were measured from two accelerometers located at 135^0 from the pump inlet and 45^0 from the pump inlet. The vibration data was recorded and used in the FDI analysis. Each turbopump was inspected after test firings and it was determined that each pump had different bearing failures and ball wear; thus, the goal of the wavelet-based FDI system was to correctly classify the different pumps to differentiate between the various faulty pumps and a normal pump.

The analysis was performed on 13.9 seconds of data collected from the accelerometer located at 135^0 from the pump inlet during the firing test at 104% rated power level. The distinct features were determined by comparing the CWTs of the normal operating turbopump against the faulty pumps. These features were then used to train a global neural network. The neural network consisted of two hidden layers and twenty-one neurons (fourteen neurons in the first layer, seven in the second layer). The neural network was trained on 130 feature vectors and classification was performed on 1391 feature vectors. The training was determined to be complete when the sum-square error goal of 0.02 was reached.

Table 3 shows a confusion matrix presenting the classification results. The normal operating pump is designated as "nor" and the faulty pumps are represented by their flight unit number. Table 3 indicates good classification results through wavelet/neural network based FDI that includes a probability of false alarm of 0.07% and a probability of missed detection of .12%, and a probability of fault misclassification of 2.19%. Important points to note here is that these results are the basic output classifications occurring every 10 ms without any deferral mechanisms or post classification algorithms performed. Simple deferral, averaging and trending techniques will provide nearly flawless detection and identification at the sacrifice of aggregating classification decisions that are occurring every 10 ms. Another, significant point is that the data was collected from physically different pumps. Hence these results illustrate the excellent performance that can be achieved using these methods when applied to different physical units of the same type (i.e., the interoperability of the FDI systems across different units is not a problem).

Gas Turbine Example: The application here focused on investigating trending and prognostics using wavelet-based methods for detecting gas turbine engine blade tip shroud failures. Endurance tests are performed on aircraft engines to evaluate and detect component failures by operating the engine at a variety of speeds over extended time intervals. During endurance testing of the F110-GE-129 at the General Electric (GE) Aircraft Engine Division, data was collected from six accelerometers. Accelerometers measuring horizontal vibrations and vertical vibrations were positioned at each of three different locations. These three locations included the front end of the fan frame, the rear end of the fan frame, and the rear end of the low pressure turbine frame (Figure 3).

TABLE 3. WAVELET / NEURAL NETWORK FDI RESULTS FOR HPOTP SSME

	Estimated Classes							
Correct Classes	nor	un2325	un2321	un2224	un2322	un4402	un4009	def
nor	1390	1	0	0	0	0	0	0
un2325	1	1334	3	18	0	20	15	0
un2321	0	2	1376	3	0	4	6	0
un2224	0	17	0	1371	0	0	3	0
un2322	3	0	0	0	1385	3	0	0
un4402	5	74	4	0	4	1293	11	0
un4009	1	10	2	0	0	4	1374	0

During the endurance tests, a shroud failure (i.e., partial separation of the shroud) occurred on a blade tip in the second stage of the low pressure turbine (LPT). This failure caused a rotor imbalance, which consequently generated engine vibrations. At the time of failure, the turbine was operating at approximately 8600 rotations per minute (rpm). GE Aircraft Division provided the raw data from all six accelerometer sites to ALPHATECH, Inc., for analysis. The purpose of the analysis was to determine whether the failure could be detected, and whether that failure could be predicted.

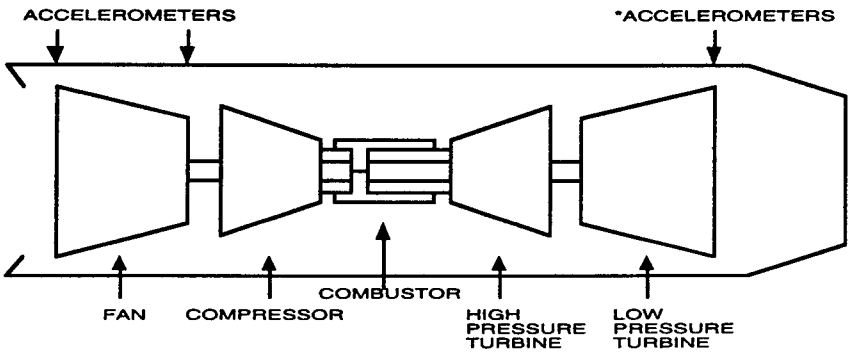

*Horizontal Accelerometer Data at this location analyzed.
(Failure at Second Stage of Low Pressure Turbine.)

Figure 3: Instrumented Turbine Engine

Analysis of the GE turbine engine data began by examining the accelerometer data from all six accelerometer locations using time-scale analysis (i.e., CWT visualizations), while considering turbine engine mechanics and general turbine engine operation. Although the time-scale analysis indicated all six sensors detected the fault, the horizontal accelerometer at the turbine fan frame location generated the most prominent reaction to the blade tip shroud failure. The attenuated response at the remote accelerometers (relative to the LPT stage 2 turbine blade) is explained by the mechanical structure of the turbine engine.

Using data from the horizontal accelerometer at the turbine frame, time-scale analysis was performed on a four second region, eighty seconds prior to the shroud failure, and a four second period, one-hundred forty-one seconds following the shroud failure. By observing the Normal (i.e., pre-failure) operation CWT and comparing with the Fault operation (i.e., post-failure) CWT, several distinguishing characteristics appear. It was thus clear from the CWT visualizations that fault detection was possible.

As mentioned previously, the turbine speed at the fault instant was 8600 rpm, or 143.3 Hz. This frequency component is noticeably affected by the shroud failure, increasing in magnitude and bandwidth in the post-failure CWT. Additionally, the second harmonic of this frequency, approximately 280 Hz, appears with increased strength in the post-failure condition. Other frequencies of interest are noted by the post-failure decreases in magnitude at approximately 250 Hz, 500 Hz, 4550 Hz, and 6800 Hz.

Although CWT visualizations indicate that wavelet technology produces information to recognize the fault scenario, being able to reliably predict an impending failure before it actually occurs is a highly desired commodity in the turbine engine diagnostic community. The information obtained by comparing pre and post-failure CWT time-scale images was therefore used to train a global neural network. Once the neural network was satisfactorily trained (i.e., sum-squared error of .02), GE data from the failure period was applied to the neural network for processing and classification. A fifty-eight second interval was selected. The blade tip shroud failure occurred at approximately fifty-one seconds into this record.

Output from the neural network occurred every 10 ms during the course of the fifty-eight seconds monitored. The raw outputs of the neural network were processed by a set of causal algorithms (i.e. algorithms that could be used in an on-line, real-time monitoring system). Figure 4 presents the results of this processing.

As the top plot (Normal Indicator) of Figure 4 illustrates, at the beginning of the fifty-eight second interval, or nearly 40 seconds before the actual failure, the system is generating a strong indication of normal activity, with no indication (bottom plot, Fault Indicator) of any fault; however, almost immediately thereafter, the Normal Indicator begins declining at approximately the same rate as the rise in the Fault Indicator, thereby illustrating a system with a progressively increasing fault. By approximately second 26 on the relative time plots, both Normal and Fault Indicators are at a value of 0.5, strongly implying a faulted system, particularly when compared to the Normal operation as evidenced at relative time 0-5 seconds. By second forty, or eleven seconds before actual failure, the Fault Indicator, at value 0.7, heavily outweighs the Normal indicator at less than 0.3. By second forty, the system outputs have moved closer spatially to the fault condition.

The trending results are extremely promising for detecting faults before actual failure. By implementing thresholding logic upon globally trained neural network data as shown in Figure 4, system operation may be accurately characterized for reliable and robust prognostic systems.

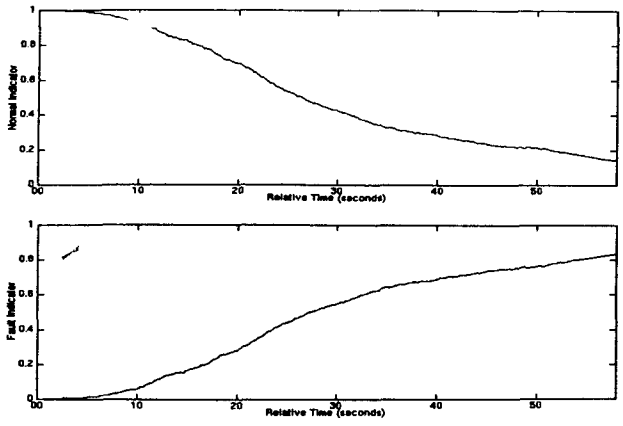

Figure 4: Fault Indicators for F110-GE-129 Turbine

SYSTEM ENHANCEMENTS: Wavelet visualizations in the form of CWTs from different sensor sites provide varying perspectives and insight into the mechanical operation of the transmission [10]. In fact, it is highly desirable to distribute the sensors around the transmission to guarantee observability of all important mechanical phenomena available from the vibration signals that could provide useful in health monitoring operations. Previous work has indicated that it is possible to achieve comparable, well performing, wavelet-based FDI systems from more than just a single sensor site [11]. An issue to consider would be how this information from multiple sensors might be combined to produce higher performing wavelet-based FDI systems.

One method for combining information from multiple sensor sites to achieve higher performing wavelet-based FDI systems would be to combine information extracted from the sensor sites at the feature vector level before performing classification. The next section on using multi-sensor wavelet-based differential features discusses such an approach and presents results achieved.

Another method for improved FDI consists of combining information from multiple sensors after the classification stage. A number of sensor sites can lead to reasonably well performing, single sensor, wavelet-based FDI systems. All such FDI systems are continuously making assessments about the operational condition of the platform (i.e., whether or not it is in a normal regime). When a failure is detected these systems, localized to an individual sensor site, are trained to decipher which particular fault the transmission is currently suffering from. However, different sites allow viewing the underlying mechanical phenomenon in different ways or from different aspects. Combining these multiple wavelet-based FDI results in some meaningful way may prove useful in developing health monitoring redundancy and increased robustness for an overall, higher performing, wavelet-based FDI system. The section dealing with hierarchical neural networks discusses one such method for combining individual sensor site wavelet / neural network FDI information for improved system performance.

Using Multi-Sensor Wavelet-Based Differential Features: To improve upon fault identification, multiple sensor wavelet extraction was investigated. The technique involves identifying a primary sensor site from which wavelet features are extracted. Using a secondary sensor site (or possibly multiple sensor sites), wavelet features at various scale settings are differenced against the primary sensor values. These differential features are conjoined to the original primary feature vector, thereby increasing its dimension. This enhanced set of feature vectors is then used as the basis for classification.

This method was applied to two channels of helicopter intermediate gearbox accelerometer data and the results were compared with results obtained using single channel data with no differential wavelet-feature augmentation. The single channel case resulted in 14 curvature/power features being extracted; however, when 15 additional differential features were added, the multiple channel case expanded to 29 curvature/power features.

To compare the separation power of the two feature sets, Fisher Linear Discriminants, which provide a one dimensional metric (linear functional) indicating the maximum separation between classes, were computed. The maximum separations computed using the differential feature element set were improved 15.2% with a resulting improvement in the FDI performance of 17.3% without deferral processing and 42.3% with deferral processing. For more details see [7].

Improved FDI Through Hierarchical Neural Networks: A natural question to be considered, in light of the fact that a select set of sensor sites have the ability to perform reasonable fault detection and identification, is the following: is there a reasonable way to combine or aggregate this FDI information from the individual sensor sites to produce a more reliable, robust, higher performing, overall FDI system? One method might be to collect the resulting FDI information from these wavelet / neural network systems and devise some ad-hoc methodology for integrating, aggregating or effectively combining the results to produce better fault detection and

identification decisions. Another method might be to defer making any decision on what this ad-hoc aggregating and/or combining algorithm should be and design a hierarchical neural network to figure out an appropriate strategy.

A hierarchical neural network would be designed to take information from a number of these complete, individual, wavelet / neural network FDI systems localized to a particular sensor. This hierarchical neural network would then be effectively trained to automatically devise an appropriate aggregation and/or combining algorithm (which could effectively be highly non-linear) to process multiple FDI data from multiple sensor sites with the goal of improving the overall robustness and performance of the eventual FDI system. Figure 5 provides a block diagram of the proposed hierarchical neural network system.

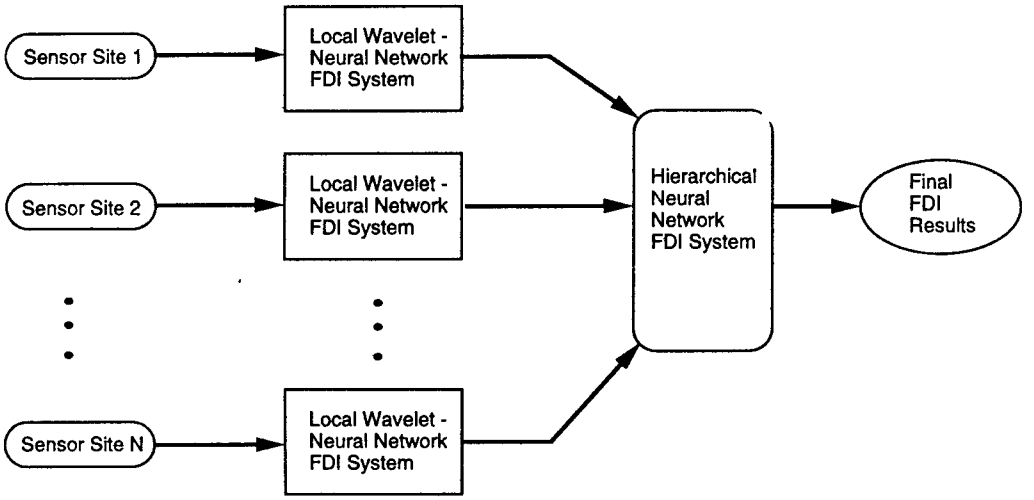

Figure 5. Block Diagram of Hierarchical Neural Network FDI System

Table 4 summarizes the neural network performance for helicopter main transmission vibration data that was recorded for normal operation and multiple fault conditions at three sensor sites. Results are given for the individual sensor wavelet/neural network FDI system (i.e., sensor 8, sensor 9, sensor 10) and the hierarchical system designed using all three sensor sites.

TABLE 4. PERFORMANCE METRICS FOR ALL FDI CONFIGURATIONS

Metric	Sensor 8	Sensor 9	Sensor 10	Sensor 8,9, & 10
PFA	0.0	0.002594	0.009079	0.0
PMD	0.003886	0.002594	0.0	0.0
PMC	0.003886	0.007782	0.01038	0.0

The networks were trained on thirty feature vectors from each fault class. Classification was conducted for each fault case across 2.52 seconds of vibration data. Table 4 shows the probability of false alarm (PFA), the probability of missed detection (PMD) and probability of misclassification (PMC). The Table 4 results indicate that the overall performance of the neural network improves as the sensor sites are combined. For more details on this methodology and simulations performed see [12].

//

CONCLUSIONS: Wavelet technology, when coupled with intelligent classification schemes constructed from neural networks, provides a basis for designing powerful fault detection and identification systems. This technology when applied to challenging vibrational systems, such as helicopter transmissions, resulted in highly accurate classification results. Similar results were obtained when applying these methods to other platforms such as turbopumps. These techniques have been extended to provide a promising prognostic / trending technique for failure prediction and fault severity indicators as demonstrated by the gas turbine application overviewed in this paper. Further robustness and improved system performance are achievable through aggregation and fusing methods across multiple sensors at both the feature extraction level and classification level. Finally, depending on the actual system requirements and needs, these basic wavelet / neural network FDI kernels, designed for real-time monitoring operations, can be integrated to support higher level diagnostic decision systems, or may be conjoined with other auxiliary information or systems in a fully integrated diagnostic/intelligent monitoring system.

REFERENCES:

1. Yan, Tinghu, Zhong, "Artificial Neural Network Technique and Its Applications to Rotating Machinery Fault Diagnosis", *J. of Vib. Engrg.*, Vol. 6, pp. 205-212, 1993.
2. Tansel, I.N., Mekdeci, C., and McLaughlin, C., "Detection of Tool Failure in End Milling With Wavelet Transformations and Neural Networks", *Manufacturing Science and Engineering ASME, Production Engineering Division*, Vol. 64, pp. 369-374, 1993.
3. Rohrbaugh, R.A., "Application of Time-Frequency Analysis to Machinery Condition Assessment", *Proc. 27th Asilomar Conf. on Sigs., Syst.* , Vol. 2, pp. 1455-1458, 1993.
4. Lopez, J.E., R.R. Tenney, and J.C. Deckert, "Wavelet Feature Extraction For Real-Time Neural Network Condition Based Maintenance," *Proc. US Navy Conference on Neural Network Applications*, Arlington, VA, 16-17 June 1994, pp. 109-121.
5. Lopez, J.E., Deckert, J.C., Tenney, R.R., "Condition-Based Machinery Maintenance: Interim Report", Alphatech, TR-663, August 1994.
6. Lopez, J.E., R.R. Tenney, and J.C. Deckert, "FDI Using Real-Time Wavelet Feature Extraction," *Proc. IEEE-SP International Symposium on Time-Frequency and Time-Scale Analysis*, Philadelphia, PA, 25-28 October 1994, pp. 217-220.
7. Lopez, J.E., R.R. Tenney, and J.C. Deckert, "Improved Fault Identification Using Multi-sensor Wavelet-Based Differential Features," *Annual Symposium on Machinery Failure Prevention Technology*, 18-20 April 1995, Virginia Beach, VA.
8. Lopez, J.E., M. Tenney, A., "Next Generation Testing and Machine Monitoring Systems Based on Application of Wavelet and Neural Network Technologies," *Test Technology Symposium XXI: Testing in lhe 21st Century*, Laurel, MD, pp. 11-13 April, 1995.
9. Lopez, J.E., Polyak, N., "Wavelet-Based Diagnostics for Helicopter Main Transmission", *American Helicopter Society 51st Annual Forum*, Fort Worth, TX, 9-11 May 1995.
10. Lopez, J.E.,"Performance of Wavelet / Neural Network Fault Detection Under Varying Operating Points", *Proceedings of the 66th Shock and Vibration Symposium,* Vol. 1, pp. 209-217, Oct.30 - Nov. 3, Biloxi, MS 1995.
11. Lopez, J.E., Oliver, K., "Improved Analysis Tools for Wavelet-Based Fault Detection", *IASTED International Conference, Signal and Image Processing - SIP- 95*, Las Vegas, NV, November 20-23, 1995.
12. Lopez, J.E., Yeldham, I.F., Oliver, K., Protz, M., "Hierarchical Neural Networks for Improved Fault Detection Using Multiple Sensors", *to be presented at the American Helicopter Society 52nd Annual Forum*, Washington, D.C., June 1996.
13. Grossman, A., R. Kronland-Martinet, and J. Morlet, "Reading and Understanding Continuous Wavelet Transforms," in *Wavelets, Time-Frequency Methods and Phase Space*, J.Combes, et. al. (Eds.), Springer-Verlag, 1989.
14. Smith, J.D., *Gears and Their Vibration*, MacMillan Press Ltd.,1983.

ACKNOWLEDGMENTS: This work was supported by the Office of Naval Research under contract N00014-93-C-0077.